

Supplementary Information

Manipulating the Lateral Diffusion of Surface-Anchored EGF Demonstrates that

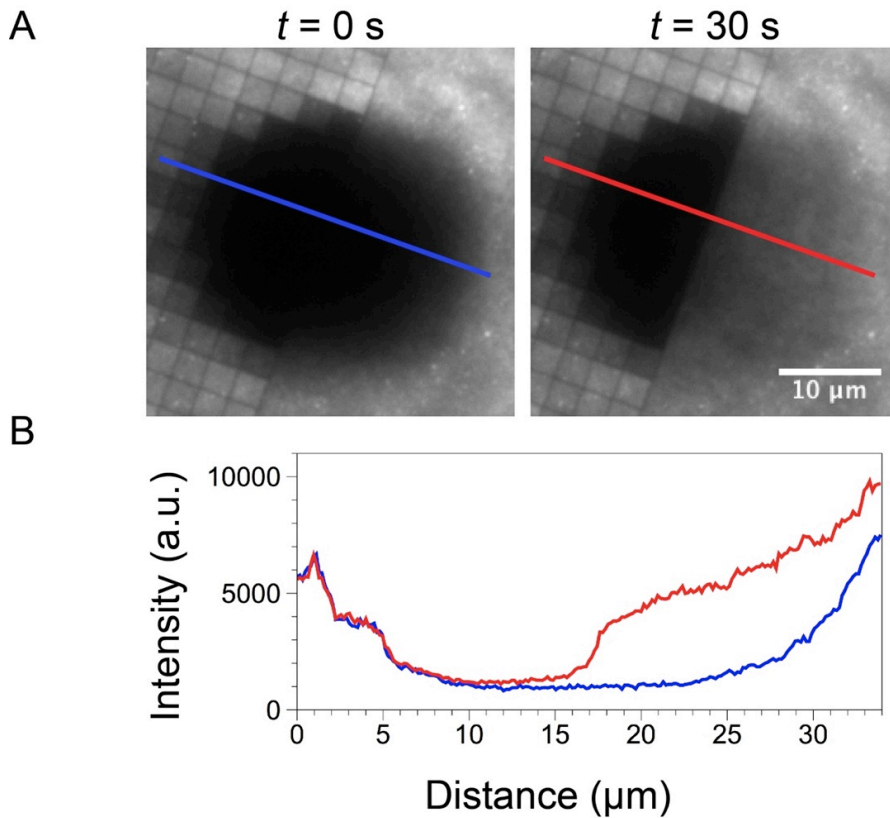
Receptor Clustering Modulates Phosphorylation Levels

D. Stabley*, S. Retterer[†], S. Marshall*, K. Salaita*

*Department of Chemistry, Emory University, Atlanta, GA

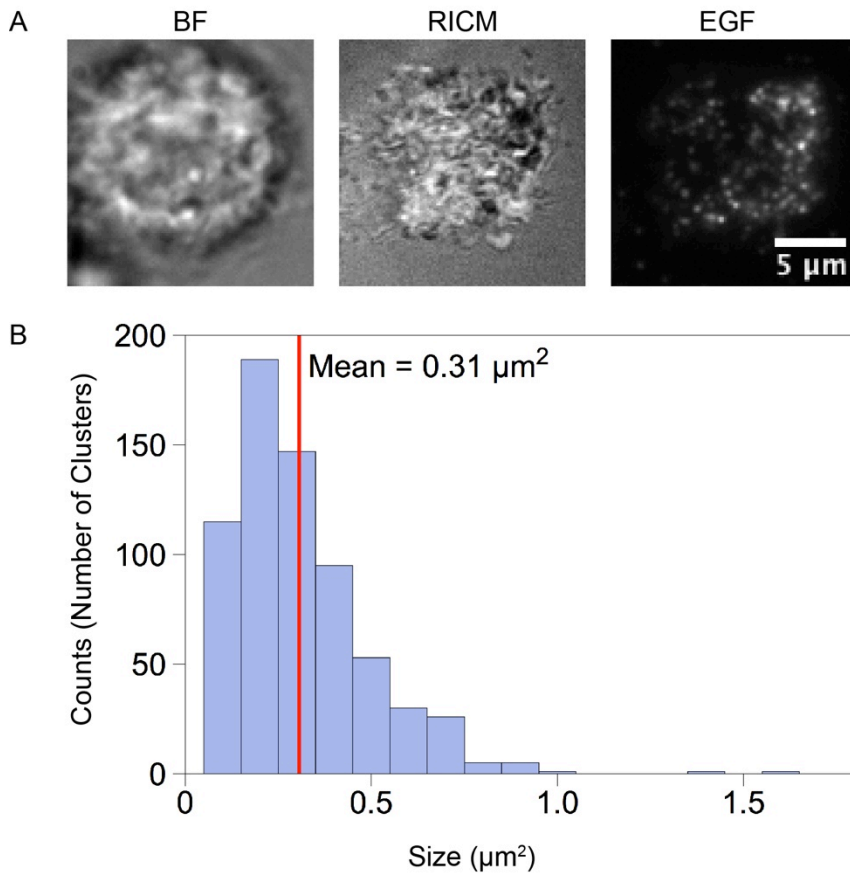
[†]Biological and Nanoscale Systems Group, Oak Ridge National Lab, Oak Ridge, TN

Supplementary Figure 1	Nanopatterns act as barriers to limit tethered-EGF diffusion.
Supplementary Figure 2	Soluble EGF stimulation leads to EGFR clustering.
Supplementary Figure 3	Schematic illustrating the image processing routine used for ratio measurement.
Supplementary Figure 4	Dimensions of nanopatterned features.
Supplementary Figure 5	Histograms showing EGF cluster size as a function of pattern type.
Supplementary Figure 6	Raw EGF, EGFR-pY1068, and EGFR Values for Figures 1 and 2.
Supplementary Figure 7	Incubation time does not significantly affect the EGFR-pY 1068/EGF ratio.
Supplementary Figure 8	EGF clusters colocalize with clathrin light chain-associated structures.



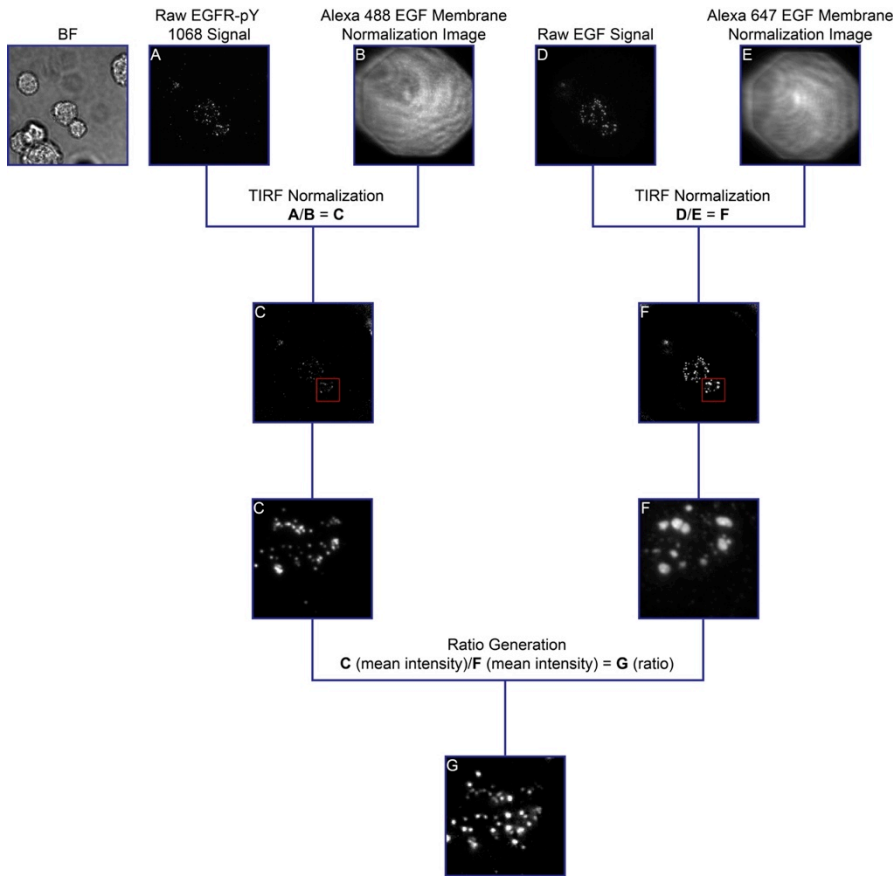
Supplementary Figure 1: Nanopatterns act as barriers to limit tethered-EGF diffusion.

(A) A fluorescence recovery after photobleaching (FRAP) experiment was performed in the TIRF 647 channel at the edge of a $3 \mu\text{m}$ grid patterned region of an EGF-Alexa 647 functionalized supported lipid bilayer (see methods for details on the preparation of supported lipid bilayers). Outside of the patterned regions, fluorescence recover is apparent due to the free diffusion of the tethered EGF-Alexa 647 conjugates. However, fluorescence recovery was abolished in the patterned region as the EGF-Alexa 647 conjugates were unable to diffuse. (B) Line scan intensity profiles of FRAP experiment indicate that recovery was primarily observed outside of the patterned region, thus showing that long-range diffusion of the EGF ligand is confined by the diffusion corrals.



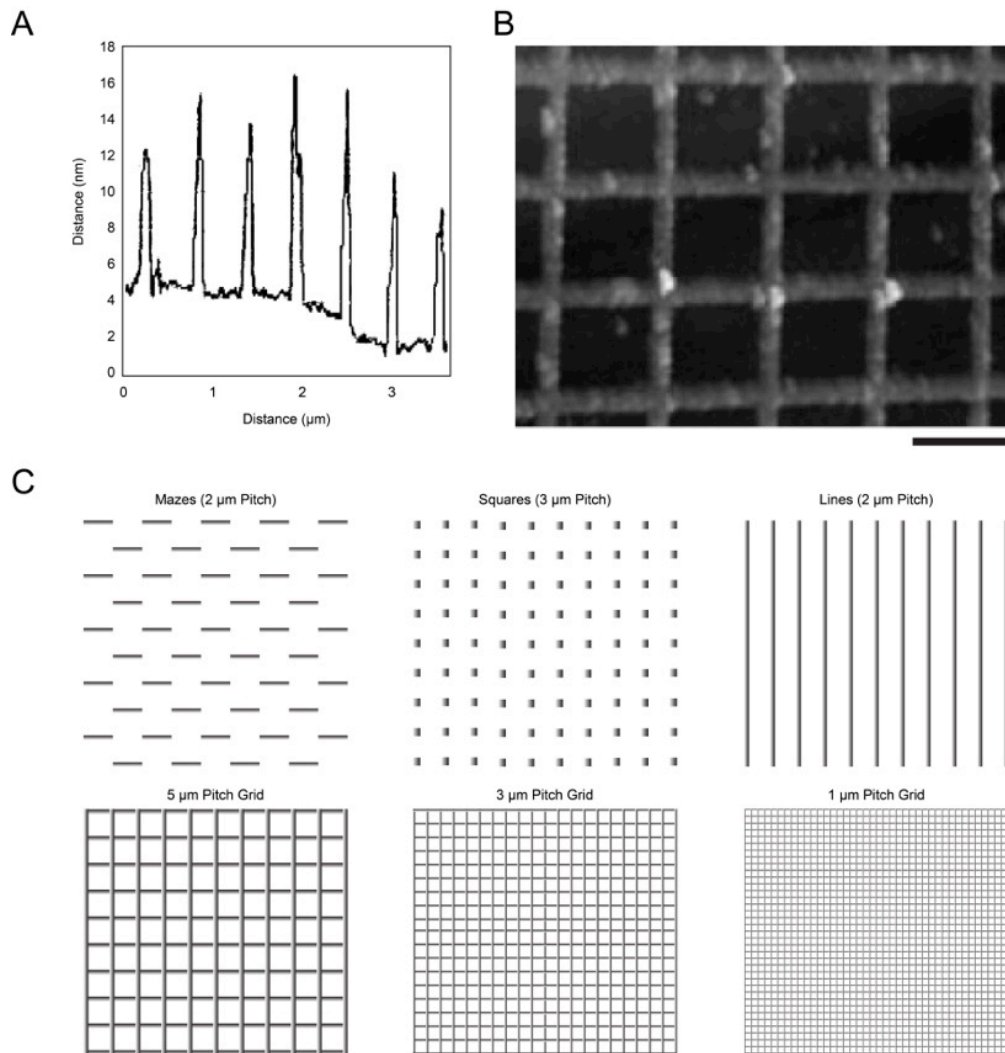
Supplementary Figure 2: Soluble EGF stimulation leads to EGFR clustering.

(A) HCC1143 cells were incubated for 1h on supported lipid membrane surfaces functionalized with cRGD peptide at 37° C, 5% CO₂. Cells were then treated with soluble EGF-Alexa 647 (1.65 nM) for 5 min and fixed. Cells exhibited clusters of EGFR, though they were generally smaller than those observed with tethered ligand. (B) Histograms of cluster size for cells in (A). Fluorescent images of EGF-647 were background subtracted and then run through an enhancement filter (Spot Tracker 2D Spot Enhancing Filter for ImageJ) after which they were subjected to binary thresholding and a watershed algorithm. Finally, particles were automatically analyzed in ImageJ (native function). $n = 668$ clusters over 5 cells.



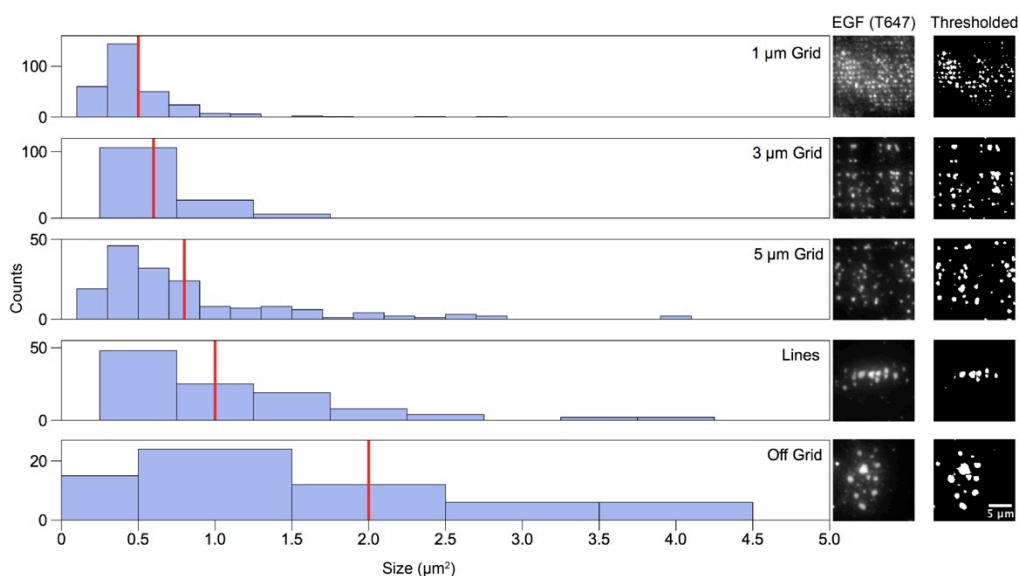
Supplementary Figure 3: Schematic illustrating the image processing routine used for ratio measurement.

After obtaining fluorescence data from cell experiments, images must be properly normalized and measured in order to yield ratio measurements of the EGFR-pY and EGF signals. First, raw fluorescence images of each channel were background subtracted. Then, each image was normalized for difference in laser excitation intensity using control fluid membranes functionalized with the dye of interest. Once the images were normalized in this manner, the mean fluorescence intensity under each individual cell was measured by placing an identical ROI over the cell of interest (note that no thresholding was used – only the raw mean fluorescence values were measured). Finally, the mean intensity from each channel was divided to yield the EGFR-pY 1068/EGF ratio.



Supplementary Figure 4: Dimensions of nanopatterned features.

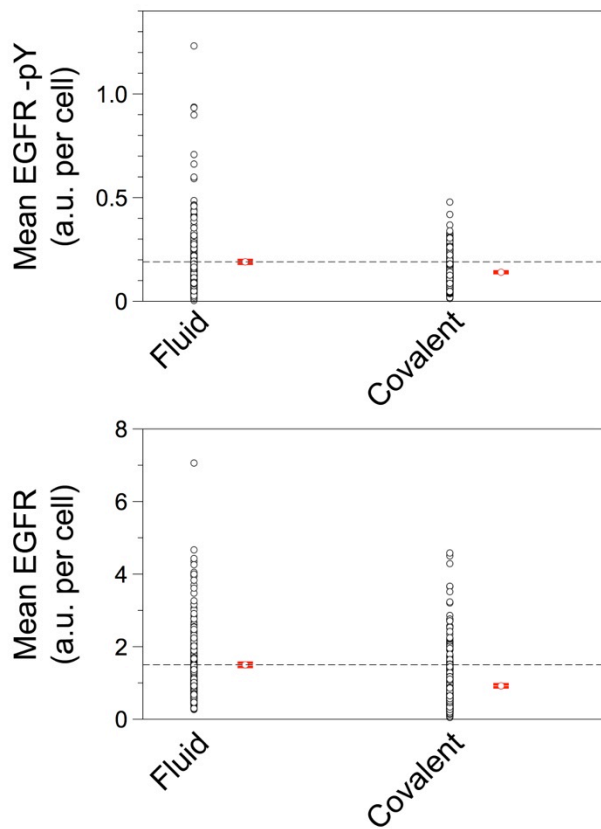
(A) Line scan taken from a representative AFM image (B) that was collected over a region of a nanopatterned grid surface with a 500 nm pitch. The line width is 110 ± 10 nm, and the line height is 10 ± 2 nm. Scale bar is 500 nm. (C) Representative schemes of the six different features used to manipulate ligand-induced EGFR clustering in live cells.



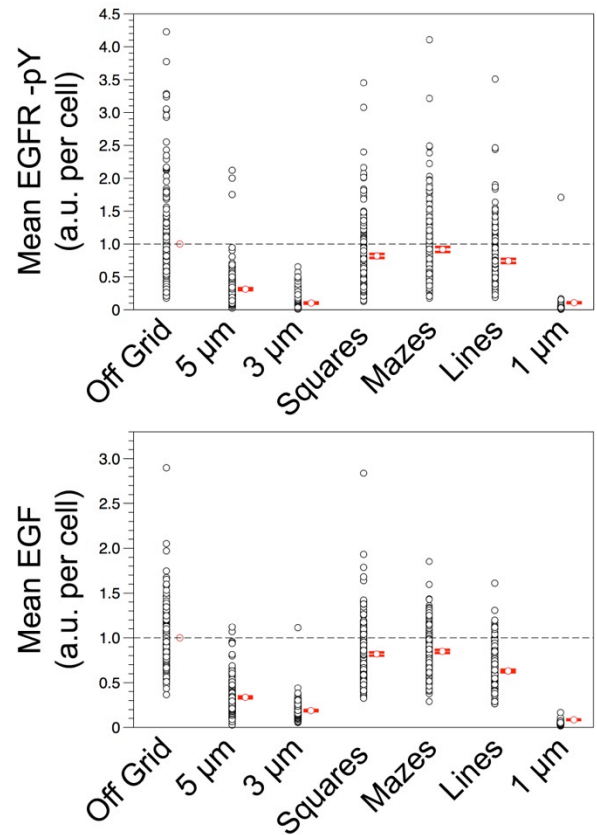
Supplementary Figure 5: Histograms showing EGF cluster size as a function of pattern type.

To estimate EGF cluster size, the raw fluorescence images collected from each nanopattern experiment were subjected to the same manual thresholding routine, resulting in a binary image delineating cluster size and location. These binary images were then automatically filtered with a watershed algorithm to reduce the number of adjacent clusters counted together during analysis. Analysis of the binary images was performed in imageJ with the standard plugin set using a $0.35 \mu\text{m}^2$ filter to prevent counting of diffraction-limited spots. Clusters for each pattern type shown were then binned according to area (red lines represent mean areas, 2, 1, 0.8, 0.6, and $0.5 \mu\text{m}^2$ for the off grid, lines, 5 μm , 3 μm , and 1 μm grids, respectively). The size of the diffusion pattern directly dictated the mean cluster area in each cell. $n = 5$ cells for the 5, 3, and 1 μm nanopatterns and 7 and 6 cells for the off grid and line patterns, respectively.

A

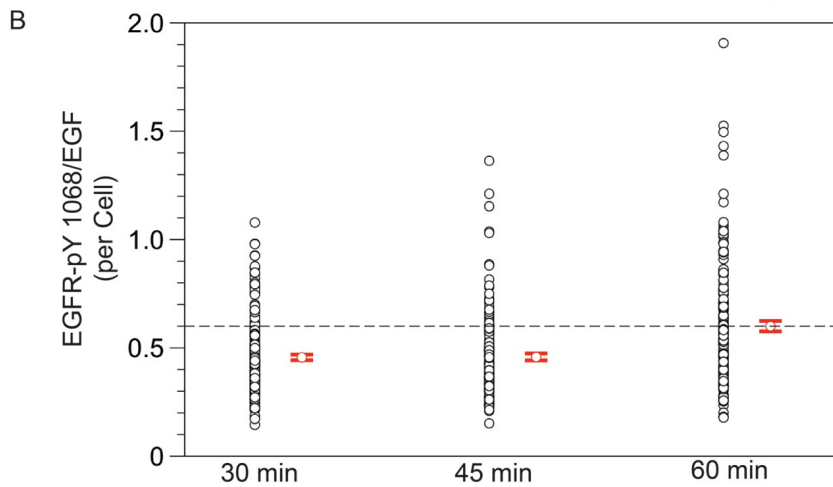
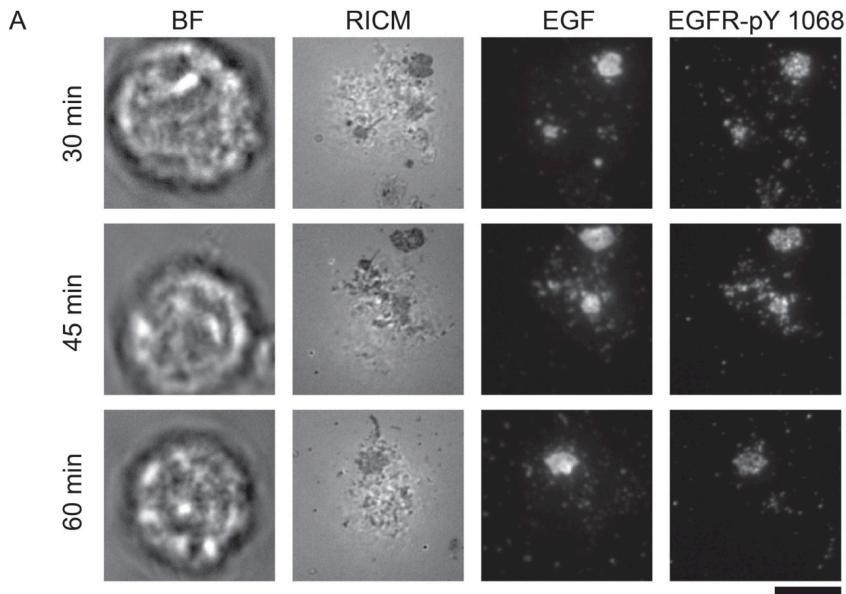


B



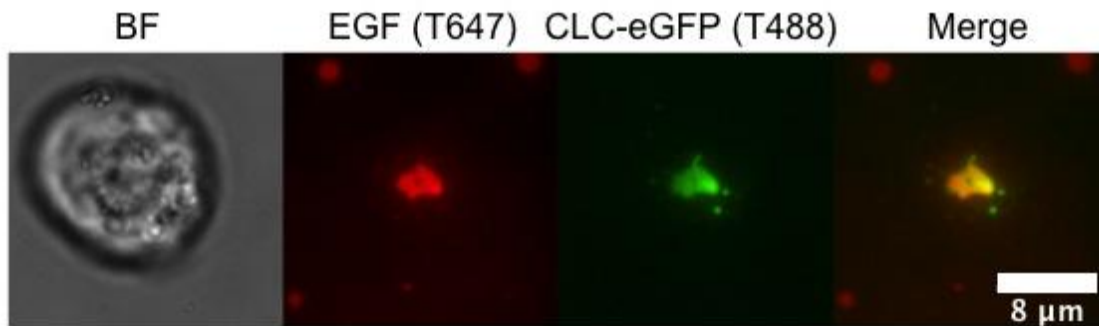
Supplementary Figure 6: Raw EGF, EGFR-pY1068, and EGFR intensity values used for ratio analysis in Figures 1 and 2.

(A) Vertical scatter plots showing the mean cell values of the EGFR-pY and EGFR signal as taken during the experiments shown in figure 1. (B) Vertical scatter plots of the mean EGFR-pY and EGF values taken under each cell during the nanopatterned supported lipid bilayer experiments shown in figure 2.



Supplementary Figure 7: Incubation time does not significantly affect the EGFR-pY 1068/EGF ratio.

(A) Representative images of HCC1143 cells that were plated onto EGF functionalized SLBs and allowed to incubate for 30, 45, and 60 minutes before fixation. The samples were then stained for EGFR-pY 1068 and imaged in the BF, RICM, EGF, and EGFR-pY 1068 channels (scale bar is 10 μ m). (B) Quantification of the EGF to EGFR-pY 1068 ratio for $n = 478$ cells revealed that there is no significant difference between the 30 and 45 min time points, and that there is a slight increase at the 60 min time point.



Supplementary Figure 8: EGF clusters colocalize with clathrin light chain-associated structures.

HCC1143 cells were transfected with a construct encoding clathrin light chain-enhanced green fluorescent protein (CLC-eGFP). After ~24 h of transfection, cells were incubated on an EGF-functionalized supported lipid bilayer for 1 h, and imaged using TIRF in the 488 and 647 nm channels. Representative brightfield, TIRF 647 (EGF), and TIRF 488 (CLC-eGFP) images, as well as an overlay of the two TIRF channels, are shown. The data indicates the formation of the characteristic EGF clusters, which were highly colocalized with clathrin assemblies.